

## The Compton amplitude and nucleon structure functions

---

**K. Utku Can<sup>a,\*</sup> for the QCDSF/UKQCD Collaboration**

<sup>a</sup>*CSSM, Department of Physics, The University of Adelaide, Adelaide SA 5005, Australia.*

*E-mail:* [kadirutku.can@adelaide.edu.au](mailto:kadirutku.can@adelaide.edu.au)

Structure functions are the essential objects for understanding the deep inelastic scattering processes, providing valuable insight into the partonic structure of hadrons. A direct calculation of the Compton amplitude provides a complementary way to accessing the structure functions, circumventing the operator mixing and renormalisation issues of the standard operator product expansion approach. We describe the connection between the Compton amplitude and the structure functions, and describe a Feynman-Hellmann approach to calculate the amplitude directly. As an application, we extract the moments of transverse and longitudinal proton structure functions and study the power corrections.

*The 39th International Symposium on Lattice Field Theory (Lattice2022),  
8-13 August, 2022  
Bonn, Germany*

---

\*Speaker

## 1. Introduction

Calculating the structure functions from first principals poses several challenges for lattice QCD practitioners. Traditionally, lattice calculations make use of the operator product (OPE) expansion. However, it is known that in the OPE approach, contributions of leading-twist operators are inseparably connected with the contributions from operators of higher twist, due to operator mixing and renormalisation [1]. In recent years, the focus has been on light-cone parton distribution functions (PDFs) accessible from the quasi-PDF approach introduced by Ji [2], which enables a direct investigation of the  $x$ -dependence of parton distributions. A detailed account of the quasi-PDF and related approaches is given in recent reviews [3, 4] and presented in plenary talks at the lattice conferences [5, 6], highlighting the immense efforts and the progress of the lattice community. The operator mixing issue, however, remains a concern [1, 7, 8]. The majority of the investigations are limited to the leading-twist contributions, with fewer works on twist-3 contributions [9–11].

In this contribution we describe an alternative and complementary approach that is being pursued by the QCDSF/UKQCD Collaboration, which is to directly calculate the forward Compton amplitude on the lattice in the space-like region. While the Compton amplitude is a 4-point correlation function, via an application of the Feynman-Hellmann approach we reduce this problem to a more straightforward analysis of 2-point functions. By working with the physical amplitude, the operator mixing and renormalization issues, and the restriction to light-cone operators are circumvented. Given the Compton amplitude is known sufficiently accurately, we can expect to estimate the power corrections in structure functions, i.e. quantify the target mass corrections and estimate the contributions from higher-twist operators, which could be useful for global PDF analyses. In principle, the  $x$ -dependence of the structure functions can be recovered [12], although in practice this requires tackling an inverse-problem [13]. Although our focus is the Compton amplitude in forward kinematics, this approach is applicable to off-forward kinematics enabling an investigation of the generalised parton distributions [14–16].

We give an overview of the relation between the Compton amplitude and the moments of structure functions in Section 2, followed by a summary of the application of the Feynman-Hellmann theorem in Section 3. The technical details follow in Sections 4 and 5. We present some selected results on the moments of nucleon structure functions and discuss the power corrections in Section 6.

## 2. The Compton tensor and the moments of structure functions

The starting point is the forward Compton amplitude described by the time ordered product of electromagnetic currents sandwiched between nucleon states,

$$T_{\mu\nu}(p, q) = \int d^4z e^{iq \cdot z} \rho_{ss'} \langle p, s' | \mathcal{T} \{ \mathcal{J}_\mu(z) \mathcal{J}_\nu(0) \} | p, s \rangle, \quad (1)$$

where  $p$  is the momentum and  $s$  is the spin of the nucleon,  $q$  is the momentum of the virtual photon, and  $\rho$  is the polarisation density matrix. For parity-conserving processes that involve conserved currents the Compton tensor is parametrised in terms of four Lorentz-invariant scalar functions,  $\mathcal{F}_1$ ,

$\mathcal{F}_2$ ,  $\mathcal{G}_1$  and  $\mathcal{G}_2$  as follows

$$T_{\mu\nu}(p, q) = T_{\{\mu\nu\}}(p, q) + T_{[\mu\nu]}(p, q) \quad (2)$$

$$T_{\{\mu\nu\}}(p, q) = \left(-g_{\mu\nu} + \frac{q_\mu q_\nu}{q^2}\right) \mathcal{F}_1(\omega, Q^2) + \left(p_\mu - \frac{p \cdot q}{q^2} q_\mu\right) \left(p_\nu - \frac{p \cdot q}{q^2} q_\nu\right) \frac{\mathcal{F}_2(\omega, Q^2)}{p \cdot q} \quad (3)$$

$$T_{[\mu\nu]}(p, q) = i\varepsilon^{\mu\nu\alpha\beta} \frac{q_\alpha}{p \cdot q} \left[ \mathcal{G}_1(\omega, Q^2) s_\beta + \mathcal{G}_2(\omega, Q^2) \left(s_\beta - \frac{s \cdot q}{p \cdot q} p_\beta\right) \right], \quad (4)$$

where we have separated the symmetric and antisymmetric parts, and  $Q^2 = -q^2$  and  $\omega = 2(p \cdot q)/Q^2$ . Here,  $\varepsilon^{0123} = 1$ , and  $s_\mu$  is the spin vector of the polarised target satisfying  $s^2 = -M^2$  ( $M$  being the mass of the nucleon) and  $s \cdot p = 0$ .

The Compton structure functions are related to the corresponding ordinary structure functions via the optical theorem, which states

$$\text{Im } \mathcal{F}_{1,2}(\omega, Q^2) = 2\pi F_{1,2}(x, Q^2), \quad (5)$$

$$\text{Im } \mathcal{G}_{1,2}(\omega, Q^2) = 2\pi g_{1,2}(x, Q^2). \quad (6)$$

Making use of analyticity, crossing symmetry and the optical theorem, we can write dispersion relations for  $\mathcal{F}$  and  $\mathcal{G}$  and connect them to the inelastic structure functions,

$$\overline{\mathcal{F}}_1(\omega, Q^2) = 2\omega^2 \int_0^1 dx \frac{2x F_1(x, Q^2)}{1 - x^2\omega^2 - i\epsilon}, \quad \mathcal{F}_2(\omega, Q^2) = 4\omega \int_0^1 dx \frac{F_2(x, Q^2)}{1 - x^2\omega^2 - i\epsilon}, \quad (7)$$

$$\mathcal{G}_1(\omega, Q^2) = 4\omega \int_0^1 dx \frac{g_1(x, Q^2)}{1 - x^2\omega^2 - i\epsilon}, \quad \mathcal{G}_2(\omega, Q^2) = 4\omega \int_0^1 dx \frac{g_2(x, Q^2)}{1 - x^2\omega^2 - i\epsilon}, \quad (8)$$

where we will use  $\overline{\mathcal{F}}_i(\omega, Q^2) = \mathcal{F}_i(\omega, Q^2) - \mathcal{F}_i(0, Q^2)$  throughout to denote a once subtracted function. Additionally, a once-subtracted dispersion relation for the longitudinal structure function  $F_L(x)$  is written as,

$$\overline{\mathcal{F}}_L(\omega, Q^2) \equiv \mathcal{F}_L(\omega, Q^2) + \mathcal{F}_L(0, Q^2) = \frac{8M_N^2}{Q^2} \int_0^1 dx F_2(x, Q^2) + 2\omega^2 \int_0^1 dx \frac{F_L(x, Q^2)}{1 - x^2\omega^2 - i\epsilon}, \quad (9)$$

where,

$$F_L(x, Q^2) = \left(1 + \frac{4M_N^2}{Q^2} x^2\right) F_2(x, Q^2) - 2xF_1(x, Q^2), \quad (10)$$

with  $M_N$  the mass of the nucleon. Note that a subtraction is necessary, given the high-energy behaviour of  $F_1$ . Although we are only concerned with subtracting it away, understanding the subtraction function is an interesting subject in itself. Related discussions on the subtraction function can be found in [17–20]. As  $Q^2 \rightarrow \infty$ , Equation (10) reduces to the familiar Callan-Gross relation,  $F_L(x) \rightarrow F_2(x) - 2xF_1(x)$ , which vanishes in the quark-parton model.

Expanding the integrands in Equations (7) to (9) at fixed  $Q^2$  as a geometric series, the Compton structure functions can be expressed as infinite sums over the Mellin moments of the inelastic

structure functions,

$$\overline{\mathcal{F}}_1(\omega, Q^2) = \sum_{n=1}^{\infty} 2\omega^{2n} M_{2n}^{(1)}(Q^2), \quad \text{with } M_{2n}^{(1)}(Q^2) = 2 \int_0^1 dx x^{2n-1} F_1(x, Q^2), \quad (11)$$

$$\mathcal{F}_2(\omega, Q^2) = \sum_{n=1}^{\infty} 4\omega^{2n-1} M_{2n}^{(2)}(Q^2), \quad \text{with } M_{2n}^{(2)}(Q^2) = \int_0^1 dx x^{2n-2} F_2(x, Q^2), \quad (12)$$

$$\overline{\mathcal{F}}_L(\omega, Q^2) = \sum_{n=1}^{\infty} 2\omega^{2n} M_{2n}^{(L)}(Q^2), \quad \text{with } M_{2n}^{(L)}(Q^2) = \int_0^1 dx x^{2n-2} F_L(x, Q^2), \quad (13)$$

$$\mathcal{G}_{1,2}(\omega, Q^2) = \sum_{n=1}^{\infty} 4\omega^{2n-1} \tilde{M}_{2n}^{(1,2)}(Q^2), \quad \text{with } \tilde{M}_{2n}^{(1,2)}(Q^2) = \int_0^1 dx x^{2n-2} g_{1,2}(x, Q^2). \quad (14)$$

We note that the physical moments  $M_{2n}$  that appear in Equations (11) to (14) are dominated by their leading-twist contributions, i.e. the moments of PDFs, at asymptotically large  $Q^2$ .

Finally, the unpolarised Compton structure functions  $\mathcal{F}_1$  and  $\mathcal{F}_2$  are accessed from the symmetric part of the Compton tensor via,

$$\mathcal{F}_1(\omega, Q^2) = T_{\{33\}}(p, q), \quad \text{for } \mu = \nu = 3 \text{ and } p_3 = q_3 = 0, \quad (15)$$

$$\frac{\mathcal{F}_2(\omega, Q^2)}{\omega} = \frac{Q^2}{2E_N^2} [T_{\{00\}}(p, q) + T_{\{33\}}(p, q)], \quad \text{for } \mu = \nu = 0 \text{ and } p_3 = q_3 = q_0 = 0, \quad (16)$$

and the longitudinal Compton structure function  $\mathcal{F}_L$  is constructed as,

$$\mathcal{F}_L(\omega, Q^2) = -\mathcal{F}_1(\omega, Q^2) + \frac{\omega}{2} \mathcal{F}_2(\omega, Q^2) + \frac{2M_N^2}{Q^2} \frac{\mathcal{F}_2(\omega, Q^2)}{\omega}. \quad (17)$$

We discuss how to access  $\mathcal{G}_1$  and  $\mathcal{G}_2$  in Section 5.

### 3. The Feynman-Hellmann technique

An analysis of the Compton amplitude requires the evaluation of lattice 4-point correlation functions. However, this is not an easy task given the rapid deterioration of the signal for large time separations and the contamination due to excited states. The application of the Feynman-Hellmann theorem reduces the problem to a simpler analysis of 2-point correlation functions using the established techniques of spectroscopy. Our implementation of the second order Feynman-Hellmann method is presented in detail in [21]. Here, we outline its main aspects.

We modify the fermion action with the following perturbing term,

$$S(\lambda) = S + \lambda \int d^3z \cos(\mathbf{q} \cdot \mathbf{z}) \mathcal{J}_\mu(z), \quad (18)$$

where  $\lambda$  is the strength of the coupling between the quarks and the external field,  $\mathcal{J}_\mu(z) = Z_V \bar{q}(z) \gamma_\mu q(z)$  is the renormalised electromagnetic current coupling to the quarks along the  $\mu$  direction,  $\mathbf{q}$  is the external momentum inserted by the current and  $Z_V$  is the renormalization constant for the local electromagnetic current. The perturbation is introduced on the valence quarks

only, hence only quark-line connected contributions are taken into account in this work. For the perturbation of valence and sea quarks see [22].

The main strategy to derive the relation between the energy shift and the matrix element is to work out the second-order derivatives of the two-point correlation function with respect to the external field from two complementary perspectives. A two-point correlation function projected to definite momentum in the presence of an external field is defined as,

$$G_\lambda^{(2)}(\mathbf{p}; t; \mathbf{\Gamma}) \equiv \int d^3x e^{-i\mathbf{p}\cdot\mathbf{x}} \mathbf{\Gamma} \langle \Omega_\lambda | \chi(\mathbf{x}, t) \bar{\chi}(0) | \Omega_\lambda \rangle, \quad (19)$$

where  $\mathbf{\Gamma}$  is the spin-parity projection matrix and  $|\Omega_\lambda\rangle$  is the vacuum in the presence of the external field. The asymptotic behaviour of the correlator at large Euclidean time takes the familiar form,

$$G_\lambda^{(2)}(\mathbf{p}; t; \mathbf{\Gamma}) \simeq A_\lambda(\mathbf{p}) e^{-E_{N_\lambda}(\mathbf{p})t}, \quad (20)$$

where  $E_{N_\lambda}(\mathbf{p})$  is the energy of the ground state nucleon in the external field and  $A_\lambda(\mathbf{p})$  the corresponding overlap factor. Differentiating the perturbed nucleon correlator (Equation (20)) with respect to energy, one finds a distinct temporal signature for the second-order energy shift,

$$\left. \frac{\partial^2 G_\lambda^{(2)}(\mathbf{p}; t)}{\partial \lambda^2} \right|_{\lambda=0} = \left( \frac{\partial^2 A_\lambda(\mathbf{p})}{\partial \lambda^2} - t A(\mathbf{p}) \frac{\partial^2 E_{N_\lambda}(\mathbf{p})}{\partial \lambda^2} \right) e^{-E_N(\mathbf{p})t}, \quad (21)$$

where we have assumed that first-order perturbations of the energy vanish, as ensured by avoiding Breit-frame kinematics. The derivatives of  $A_\lambda(\mathbf{p})$  and  $E_{N_\lambda}(\mathbf{p})$  are assumed to be evaluated at  $\lambda = 0$ . The first term corresponds to the shift in the overlap factor and the second order energy shift is identified in the  $t$ -enhanced (or time-enhanced) term.

By differentiating Equation (19) twice with respect to  $\lambda$  in the path integral formalism and evaluated at  $\lambda \rightarrow 0$ , we find

$$\left. \frac{\partial^2 G_\lambda^{(2)}(\mathbf{p}; y)}{\partial \lambda^2} \right|_{\lambda=0} = \int d^3x e^{-i\mathbf{p}\cdot\mathbf{x}} \mathbf{\Gamma} \left[ \left\langle \chi(\mathbf{x}, t) \bar{\chi}(0) \left( \frac{\partial S(\lambda)}{\partial \lambda} \right)^2 \right\rangle + \dots \right], \quad (22)$$

where ellipsis denote the terms that do not lead to a time-enhanced term. Inserting the explicit form of the external electromagnetic current (Equation (18)) and following the algebra, we arrive at,

$$\left. \frac{\partial^2 G_\lambda^{(2)}(\mathbf{p}; t)}{\partial \lambda^2} \right|_{\lambda=0} = t A(\mathbf{p}) \frac{e^{-E_N(\mathbf{p})t}}{2E_N(\mathbf{p})} \left\langle N(\mathbf{p}) \left| \int d^4z (e^{iq\cdot z} + e^{-iq\cdot z}) \mathcal{J}_\mu(z) \mathcal{J}_\mu(0) \right| N(\mathbf{p}) \right\rangle + \dots, \quad (23)$$

where the subleading terms are suppressed by the ellipsis.

Finally, matching the time-enhanced terms of this form with Equation (21), one arrives at the desired relation between the energy shift and the matrix element describing the Compton amplitude,

$$\left. \frac{\partial^2 E_{N_\lambda}(\mathbf{p})}{\partial \lambda^2} \right|_{\lambda=0} = - \frac{T_{\mu\mu}(p, q) + T_{\mu\mu}(p, -q)}{2E_N(\mathbf{p})}, \quad (24)$$

where  $T$  is the Compton amplitude defined in Equation (1). Equation (24) is the principal relation

that we use to access the flavour-diagonal, i.e.  $uu$  and  $dd$ , pieces of the symmetric part (Equation (3)) of the Compton amplitude.

The above derivation can be generalised to mixed currents by including additional perturbing terms in Equation (18) to study the flavour-mixed, i.e.  $ud$ , piece, and the antisymmetric part (Equation (4)) of the Compton tensor. On that account, we make the modifications,

$$S(\lambda) = S + \lambda_1 \int d^3z \cos(\mathbf{q} \cdot \mathbf{z}) \mathcal{J}_\mu(z) + \lambda_2 \int d^3y \cos(\mathbf{q} \cdot \mathbf{y}) \mathcal{J}_\mu(y), \quad (25)$$

$$S(\lambda) = S + \lambda_1 \int d^3z \cos(\mathbf{q} \cdot \mathbf{z}) \mathcal{J}_\mu(z) + \lambda_2 \int d^3y \sin(\mathbf{q} \cdot \mathbf{y}) \mathcal{J}_\nu(y), \quad (26)$$

to access the flavour-mixed and flavour-diagonal antisymmetric pieces of the amplitude, respectively. Consequently, expressions analogous to Equation (24) are,

$$\left. \frac{\partial^2 E_{N_\lambda}(\mathbf{p})}{\partial \lambda_1 \partial \lambda_2} \right|_{\lambda=0} = -\frac{T_{\mu\mu}(p, q) + T_{\mu\mu}(p, -q)}{2E_N(\mathbf{p})}, \quad (27)$$

$$\left. \frac{\partial^2 E_{N_\lambda}(\mathbf{p})}{\partial \lambda_1 \partial \lambda_2} \right|_{\lambda=0} = \frac{T_{\mu\nu}(p, q) - T_{\mu\nu}(p, -q)}{2E_N(\mathbf{p})}, \quad (28)$$

corresponding to the modifications in Equations (25) and (26), respectively, where the crossing relations  $T_{\mu\mu}(p, q) = T_{\mu\mu}(p, -q)$  and  $T_{\mu\nu}(p, q) = -T_{\mu\nu}(p, -q)$  ensure that we have non-vanishing Feynman-Hellmann relations.

#### 4. Extracting the energy shifts

We can expand the perturbed energy in the limit  $\lambda \rightarrow 0$ ,

$$E_{N_\lambda}(\mathbf{p}) = E_N(\mathbf{p}) + \lambda \left. \frac{\partial E_{N_\lambda}(\mathbf{p})}{\partial \lambda} \right|_{\lambda=0} + \frac{\lambda^2}{2!} \left. \frac{\partial^2 E_{N_\lambda}(\mathbf{p})}{\partial \lambda^2} \right|_{\lambda=0} + O(\lambda^3) \quad (29)$$

$$= E_N(\mathbf{p}) + \Delta E_{N_\lambda}^e(\mathbf{p}) + \Delta E_{N_\lambda}^o(\mathbf{p}), \quad (30)$$

considering a single current insertion (e.g. Equation (18)), where we have collected the terms even ( $e$ ) and odd ( $o$ ) in  $\lambda$  to all orders in writing the second line. A similar Taylor expansion of the perturbed energy can be written for the double current insertion (e.g. Equation (25)),

$$E_{N_\lambda}(\mathbf{p}) = E_N(\mathbf{p}) + \Delta E_{N_\lambda}^{eo}(\mathbf{p}) + \Delta E_{N_\lambda}^{oe}(\mathbf{p}) + \Delta E_{N_\lambda}^{ee}(\mathbf{p}) + \Delta E_{N_\lambda}^{oo}(\mathbf{p}), \quad (31)$$

where the term of interest is,

$$\Delta E_{N_\lambda}^{oo}(\mathbf{p}) = \lambda_1 \lambda_2 \left. \frac{\partial^2 E_{N_\lambda}(\mathbf{p})}{\partial \lambda_1 \partial \lambda_2} \right|_{\lambda=0} + O(\lambda_1 \lambda_2^3) + O(\lambda_1^3 \lambda_2), \quad (32)$$

with respect to Equations (27) and (28).

We construct the ratios,

$$\mathcal{R}_\lambda^e(\mathbf{p}; t; \Gamma_4) \equiv \frac{G_{+\lambda}^{(2)}(\mathbf{p}; t; \Gamma_4) G_{-\lambda}^{(2)}(\mathbf{p}; t; \Gamma_4)}{(G^{(2)}(\mathbf{p}; t; \Gamma_4))^2} \xrightarrow{t \gg 0} A_\lambda(\mathbf{p}) e^{-2\Delta E_{N_\lambda}^e(\mathbf{p}) t}, \quad (33)$$

$$\mathcal{R}_\lambda^{oo}(\mathbf{p}; t; \Gamma) \equiv \frac{G_{(+\lambda, +\lambda)}^{(2)}(\mathbf{p}; t; \Gamma) G_{(-\lambda, -\lambda)}^{(2)}(\mathbf{p}; t; \Gamma)}{G_{(+\lambda, -\lambda)}^{(2)}(\mathbf{p}; t; \Gamma) G_{(-\lambda, +\lambda)}^{(2)}(\mathbf{p}; t; \Gamma)} \xrightarrow{t \gg 0} A_\lambda(\mathbf{p}) e^{-4\Delta E_{N_\lambda}^{oo}(\mathbf{p}) t}, \quad (34)$$

in order to extract the second-order energy shifts, where  $A_\lambda(\mathbf{p})$  is the overlap factor, which is irrelevant for the rest of the discussion. These ratios isolate the energy shifts only at even orders of  $\lambda$ . Here,  $G_\lambda^{(2)}$  and  $G_{(\lambda_1, \lambda_2)}^{(2)}$  are the perturbed two-point functions with  $|\lambda_1| = |\lambda_2| = |\lambda|$ , and  $G^{(2)}$  is the unperturbed one. The spin-parity projection matrices are defined as  $\Gamma_4 \equiv (1 + \gamma_4)/2$  for an unpolarised positive-parity nucleon, and  $\Gamma_+^\hat{e} \equiv \Gamma_4(1 + \hat{e} \cdot \boldsymbol{\gamma} \gamma_5)/2$  for a spin-up positive-parity nucleon polarised along the  $\hat{e}$  direction. Equation (33) is used for the flavour-diagonal pieces of the symmetric part of the Compton amplitude, i.e.  $\mathcal{F}_{(1,2)}^{(uu,dd)}$ , while Equation (34) with  $\Gamma = \Gamma_4$  is used for the flavour-mixed piece, i.e.  $\mathcal{F}_{(1,2)}^{ud}$ .

## 5. Separating the $\mathcal{G}_1$ and $\mathcal{G}_2$

Accessing the polarised Compton structure functions  $\mathcal{G}_1$  and  $\mathcal{G}_2$  is more involved. By choosing the currents along the  $\mu = 1$ , and  $\nu = 2$  directions, and adopting the kinematics  $q_1 = p_1 = 0$ , we cancel the symmetric part (Equation (3)) and isolate the spin dependent part of the tensor,

$$T_{[12]}(p, q) = i\varepsilon^{1230} \frac{q_3}{p \cdot q} \left[ \mathcal{G}_1(\omega, Q^2) s_0 + \mathcal{G}_2(\omega, Q^2) \left( s_0 - \frac{s \cdot q}{p \cdot q} p_0 \right) \right], \quad (35)$$

where we are left with the choices  $\alpha = 3$  and  $\beta = 0$  to have a non-vanishing amplitude since  $q_0 = 0$  by construct in the Feynman-Hellmann approach. We rearrange Equation (35) by using the four-spin vector in a boosted frame,

$$s^\mu(\mathbf{p}) \equiv \left( \frac{\hat{e} \cdot \mathbf{p}}{M_N}, \hat{e} + \frac{\hat{e} \cdot \mathbf{p}}{M_N(E_N(\mathbf{p}) + M_N)} \mathbf{p} \right), \quad (36)$$

where  $\hat{e} = \sigma M_N \hat{n}$ , with  $\hat{n}$  the quantisation axis and  $\sigma = +1$  for spin up, along with the substitutions  $\varepsilon^{0123} = 1$ ,  $p_0 = E_N(\mathbf{p})$ ,  $a \cdot q \equiv a^\mu q_\mu = -\mathbf{a} \cdot \mathbf{q}$ , and  $\omega = 2(\mathbf{p} \cdot \mathbf{q})/Q^2$ , into a more compact form,

$$T_{[12]}^\hat{e}(p, q) = C_1(\hat{e}, \mathbf{p}, \mathbf{q}) \frac{\mathcal{G}_1(\omega, Q^2)}{\omega} + C_2(\hat{e}, \mathbf{p}, \mathbf{q}) \frac{\mathcal{G}_2(\omega, Q^2)}{\omega}, \quad (37)$$

with the coefficients,

$$C_1(\hat{e}, \mathbf{p}, \mathbf{q}) = i \frac{2q_3}{Q^2} \frac{\hat{e} \cdot \mathbf{p}}{M_N}, \quad (38)$$

$$C_2(\hat{e}, \mathbf{p}, \mathbf{q}) = i \frac{2q_3}{Q^2} \left[ \frac{\hat{e} \cdot \mathbf{p}}{M_N} - E_N(\mathbf{p}) \left( \frac{\hat{e} \cdot \mathbf{p}}{M_N(E_N(\mathbf{p}) + M_N)} + \frac{\hat{e} \cdot \mathbf{q}}{\mathbf{p} \cdot \mathbf{q}} \right) \right]. \quad (39)$$

Note that we have introduced a superscript  $\hat{e}$  in Equation (37) to keep track of the spin polarisations. Once we extract the energy shifts,  $\Delta E_{N_\lambda}^{oo}(\mathbf{p})$ , using Equation (34) with  $\mathbf{\Gamma} = \mathbf{\Gamma}_+^{\hat{e}}$  and  $\hat{e}$  along the  $\hat{y}$  and  $\hat{z}$  directions, and determine the Compton amplitude using Equation (28), we separate  $\mathcal{G}_1$  and  $\mathcal{G}_2$  by solving the system of linear equations,

$$\mathbf{T} = \mathbf{C} \mathbf{g}, \quad (40)$$

where  $\mathbf{T} = [T_{[12]}^{\hat{y}}, T_{[12]}^{\hat{z}}]^\top$ ,  $\mathbf{g} = [\mathcal{G}_1, \mathcal{G}_2]^\top / \omega$ , and the coefficient matrix

$$\mathbf{C} = \begin{pmatrix} C_1(\hat{y}, \mathbf{p}, \mathbf{q}) & C_2(\hat{y}, \mathbf{p}, \mathbf{q}) \\ C_1(\hat{z}, \mathbf{p}, \mathbf{q}) & C_2(\hat{z}, \mathbf{p}, \mathbf{q}) \end{pmatrix}. \quad (41)$$

## 6. Selected results and discussion

We first present our results for the unpolarised Compton amplitude. Our simulations are carried out on QCDSF/UKQCD-generated 2 + 1-flavour gauge configurations. Two ensembles are used with volumes  $V = [32^3 \times 64, 48^3 \times 96]$ , and couplings  $\beta = [5.50, 5.65]$  corresponding to lattice spacings  $a = [0.074, 0.068]$  fm, respectively. Quark masses are tuned to the  $SU(3)$  symmetric point where the masses of all three quark flavours are set to approximately the physical flavour-singlet mass,  $\bar{m} = (2m_s + m_l)/3$  [23, 24], yielding  $m_\pi \approx [470, 420]$  MeV. Up to  $\mathcal{O}(10^4)$  and  $\mathcal{O}(10^3)$  measurements are performed by employing multiple sources on the  $32^3 \times 64$  and  $48^3 \times 96$  ensembles, respectively.

We obtain amplitudes for several values of current momentum,  $Q^2$ , in the range  $1.5 \lesssim Q^2 \lesssim 7$   $\text{GeV}^2$ . Multiple  $\omega$  values are accessed at each simulated value of  $\mathbf{q}$  by varying the nucleon momentum  $\mathbf{p}$ , which allows for a mapping of the  $\omega$  dependence of the Compton structure functions. For each  $\omega$ , we extract the energy shifts from the ratios defined in Equations (33) and (34) for two  $|\lambda|$  values. We determine the fit windows by a covariance-matrix based  $\chi^2$  analysis where we choose the ranges that have  $\chi_{dof}^2 \sim 1.0$ . Effective mass plots for the ratios are shown in Figure 1 for some selected cases.

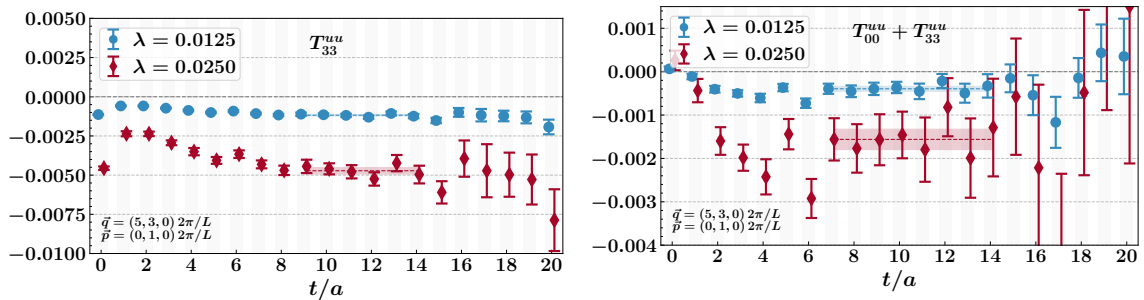


**Figure 1:** Effective mass plots of the ratios (Equation (33)) for the amplitudes  $T_{33}$  (left) and  $T_{00} + T_{33}$  (right). Fit windows, along with the extracted energy shifts with their  $1\sigma$  uncertainty, are shown by the shaded bands. We are showing the results obtained on the  $48^3 \times 96$  ensemble for the  $uu$  piece, for  $(\mathbf{p}, \mathbf{q}) = ((0, 1, 0), (5, 3, 0)) \left(\frac{2\pi}{L}\right)$  corresponding to  $\omega = 0.18$  at  $Q^2 \sim 4.9 \text{ GeV}^2$ . Figures taken from [25].



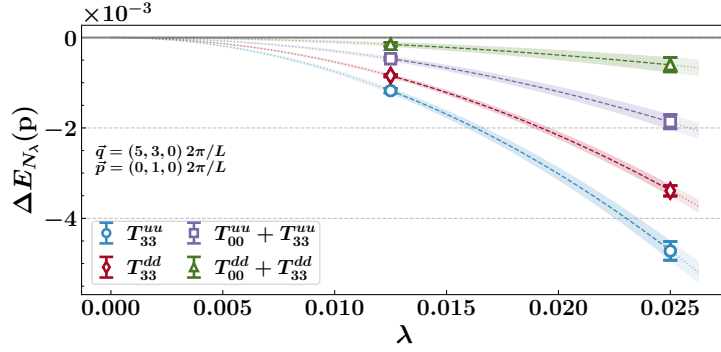


**Figure 2:**  $\lambda$  dependence of the energy shifts for the  $uu$  and  $dd$  pieces of the  $T_{33}$  and  $T_{00} + T_{33}$  amplitudes. Results are from the  $48^3 \times 96$  ensemble with the same kinematics given in Figure 1. Figure taken from [25].

We perform polynomial fits of the form,  $\Delta E_{N_\lambda}(\mathbf{p}) = \lambda^2 \left. \frac{\partial^2 E_{N_\lambda}(\mathbf{p})}{\partial \lambda^2} \right|_{\lambda=0} + O(\lambda^4)$ , to determine the second order energy shift. Equation (32) also reduces to this form since we set  $|\lambda_1| = |\lambda_2| = |\lambda|$  in our simulations. The unperturbed energy,  $E_N$ , and odd-order lambda terms ( $O(\lambda)$ ,  $O(\lambda^3)$ , ...) are removed by construction in the ratios. Given the smallness of our  $\lambda$  values, higher order  $O(\lambda^4)$  terms are heavily suppressed, hence the fit form reduces to a simple one parameter polynomial. We show representative cases for the  $\lambda$  fits in Figure 2. We confirm the suppression of the  $O(\lambda^4)$  term, and the absence of  $\lambda$ -odd terms, by including  $O(\lambda)$ ,  $O(\lambda^3)$ , and  $O(\lambda^4)$  terms separately in the fit. We find that any residual contamination has a negligible effect compared to the statistical error on the extracted amplitudes.

The above analysis is performed to map out the  $\omega$  dependence of the Compton structure functions given in Equations (15) and (16) for each  $Q^2$  value that we study.  $\mathcal{F}_L(\omega, Q^2)$  is constructed according to Equation (17). We show the  $\omega$  dependence of the Compton structure functions, along with their fit curves, in Figure 3 for a representative case of  $Q^2 \sim 4.9 \text{ GeV}^2$  calculated on the  $48^3 \times 96$  ensemble.

The first few Mellin moments of  $F_1$ ,  $F_2$  and  $F_L$  are determined by performing a simultaneous fit to  $\overline{\mathcal{F}}_1$  and  $\mathcal{F}_2$  in a Bayesian framework at each  $Q^2$  value. We use Equation (11) for  $\overline{\mathcal{F}}_1$  and express  $\mathcal{F}_2$  in terms of the independently positive definite moments of  $F_1$  and  $F_L$ ,

$$\frac{\mathcal{F}_2(\omega)}{\omega} = \frac{\tau}{(1 + \tau \omega^2)} \sum_{n=0}^{\infty} 4\omega^{2n} \left[ M_{2n}^{(1)} + M_{2n}^{(L)} \right], \quad (42)$$

where  $\tau = Q^2/4M_N^2$ ,  $M_0^{(1)}(Q^2) = 0$ , and  $M_0^{(L)}(Q^2) = \frac{4M_N^2}{Q^2} M_2^{(2)}(Q^2)$ . The intercept at  $\omega = 0$  is proportional to the lowest moment of  $F_2$ , i.e.  $M_2^{(2)}(Q^2)$ . We truncate the series at  $n = 4$  (inclusive). No dependence on higher-order terms is seen. We sample the moments from uniform distributions with bounds  $M_2(Q^2) \in [0, 1]$  and  $M_{2n}(Q^2) \in [0, M_{2n-2}(Q^2)]$ , for  $n > 1$ , to enforce the monotonic decreasing nature of the moments,  $M_2(Q^2) \geq M_4(Q^2) \geq \dots \geq M_{2n}(Q^2) \geq \dots \geq 0$ , for  $uu$  and  $dd$  contributions separately. Note that the positivity bound does not hold for the  $ud$  contributions but they are constrained by  $|M_{2n}^{ud}(Q^2)|^2 \leq 4M_{2n}^{uu}(Q^2)M_{2n}^{dd}(Q^2)$ , since the total inclusive cross section (hence each moment) is positive for any value of the quark charges and at all kinematics. The

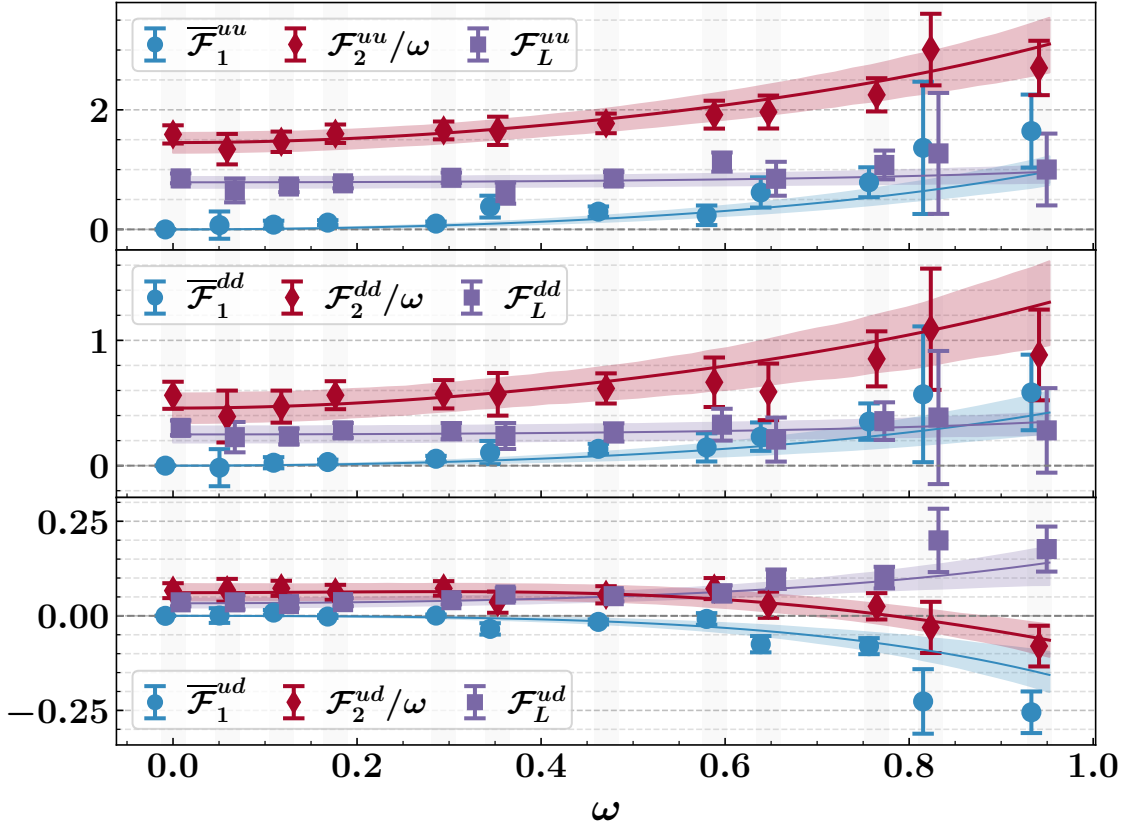


**Figure 3:**  $\omega$  dependence of the Compton structure functions  $\overline{\mathcal{F}}_1$ ,  $\mathcal{F}_2$ , and  $\overline{\mathcal{F}}_L$  at  $Q^2 \sim 4.9 \text{ GeV}^2$  for the  $uu$  (top),  $dd$  (middle) and  $ud$  (bottom) contributions. Coloured shaded bands show the fits with their 68% credible region of the highest posterior density. Points are displaced for clarity. Figure taken from [25].

sequences of individual  $uu$ ,  $dd$ , and  $ud$  moments are selected according to the standard probability distribution,  $\exp(-\chi^2/2)$ , where,  $\chi^2 = \sum_{\mathcal{F}} \sum_i [\mathcal{F}_i^{\text{model}} - \mathcal{F}_i^{\text{obs}}(\omega_i)]^2 / \sigma^2$ , is the  $\chi^2$  function with  $\sigma^2$  the diagonal elements of the full covariance matrix. Here,  $\mathcal{F}$  stands for  $\overline{\mathcal{F}}_1$  and  $\mathcal{F}_2$ , and the indices  $i, j$  run through all the  $\omega$  values and flavour-diagonal and mixed-flavour pieces. We account for the correlations between the data points by a bootstrap analysis. Fits depicting the extraction of the moments are also shown in Figure 3 by shaded bands for a representative case.

We show the lowest moments of  $F_2$  for proton in Figure 4 as a function of  $Q^2$ . Note that the moments of the proton are constructed via  $M_{2,p}^{(2,L)} = \frac{4}{9}M_{2,uu}^{(2,L)} + \frac{1}{9}M_{2,dd}^{(2,L)} - \frac{2}{9}M_{2,ud}^{(2,L)}$ . Also shown are the experimental determinations of the Cornwall-Norton moments of  $F_2$  [26]. We see a remarkable agreement, although we should note that our systematics are not fully accounted for yet.

The Compton amplitude encompasses all power corrections, therefore it is possible to estimate the leading power correction (i.e. twist-4) by studying the  $Q^2$  behaviour of the moments in a twist expansion,

$$M_{2,h}^{(2)}(Q^2) = M_{2,h}^{(2)} + C_{2,h}^{(2)}/Q^2 + \mathcal{O}(1/Q^4), \quad (43)$$

where  $h \in \{uu, dd, ud, p\}$ . Utilising only the  $M_2^{(2)}(Q^2)$  moments obtained on the  $48^3 \times 96$  ensemble, we study the power corrections down to  $Q^2 \approx 1.5 \text{ GeV}^2$ . Our fit for proton is shown

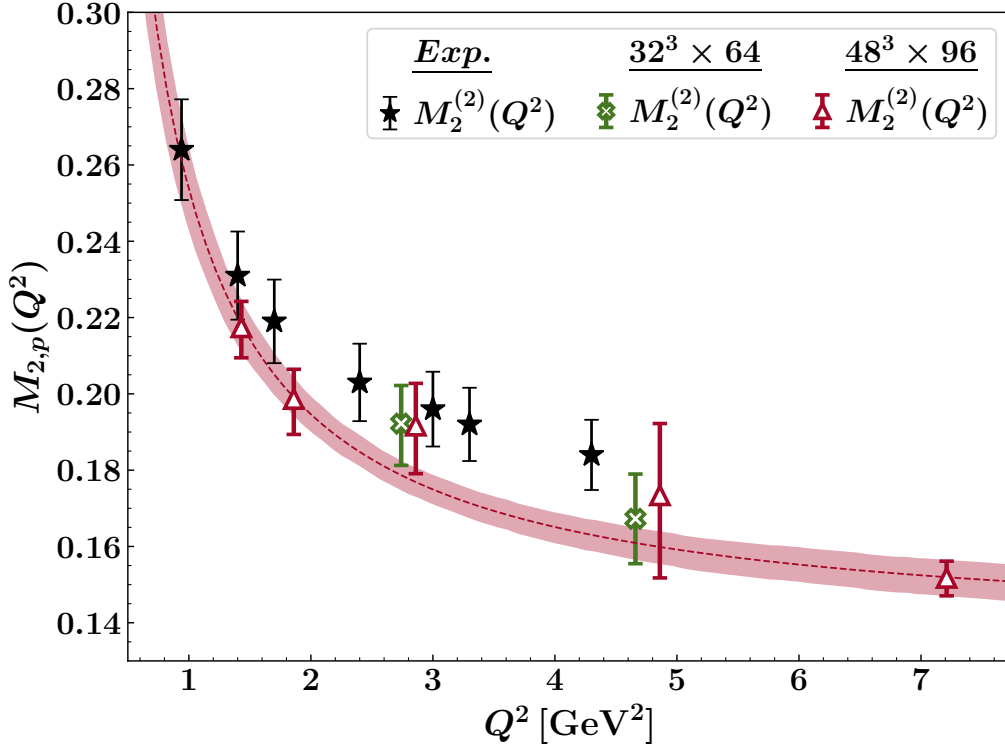


**Figure 4:**  $Q^2$  dependence of the lowest moments of proton  $F_2$ . Filled stars are the experimental Cornwall-Norton moments of  $F_2$  [26]. Figure taken from [25].

in Figure 4. The extracted values for  $M_{2,h}^{(2)}$  and  $C_{2,h}^{(2)}$  are collected in Table 1. Although we focus on the proton due to availability of experimental data, it is possible to estimate the moments for neutron or the isovector  $u - d$  combination since we have the contributions of different flavour components. Power corrections are a combination of target mass corrections, pure higher-twist terms, and the elastic contributions. These effects can be disentangled further, for instance by determining the elastic contributions from form factors [27, 28], and employing Nachtmann moments [29] to account for the target mass corrections, along with including the logarithmic evolution of moments in Equation (43). We leave such an investigation to a future study.

**Table 1:** Asymptotic values of the moments and the coefficients of the leading power correction terms. We quote the power corrections at the scale of the nucleon mass  $Q^2 = M_N^2$ .

$h$	$M_{2,h}^{(2)}$	$C_{2,h}^{(2)}/M_N^2$
$uu$	0.268(13)	0.206(24)
$dd$	0.146(7)	0.024(14)
$ud$	0.000(0)	0.007(3)
$p$	0.135(6)	0.091(11)

In Figure 5, we show the lowest (Cornwall-Norton) moments of  $F_L$  in comparison to the experimentally determined Nachtmann moments [30]. With our current precision, we are able to set an upper bound for the moments that is compatible with the experimental moments.

The leading twist part of  $F_L$  is related to  $F_2$  in leading-order in  $\alpha_s$ . In terms of moments this relation reads [31],

$$M_{2,p}^{(L),\text{twist}-2}(Q^2) = \frac{4}{9\pi} \alpha_s(Q^2) M_{2,p}^{(2),\text{twist}-2}(Q^2), \quad (44)$$

where we have replaced the leading-twist moment on RHS with  $M_{2,p}^{(2)}(Q^2)$  from the current work as an approximation. We use the value of  $\alpha_s(Q^2)$  determined in the  $\overline{MS}$  scheme at  $\mu = Q^2$  at the four-loop order. The  $Q^2$  behaviour is in good agreement with experimental points as shown in Figure 5. Improving the precision in future studies, would help to resolve the difference between the direct determination and twist-2 part of the lowest few moments of  $F_L$  and reveal the higher-twist effects.

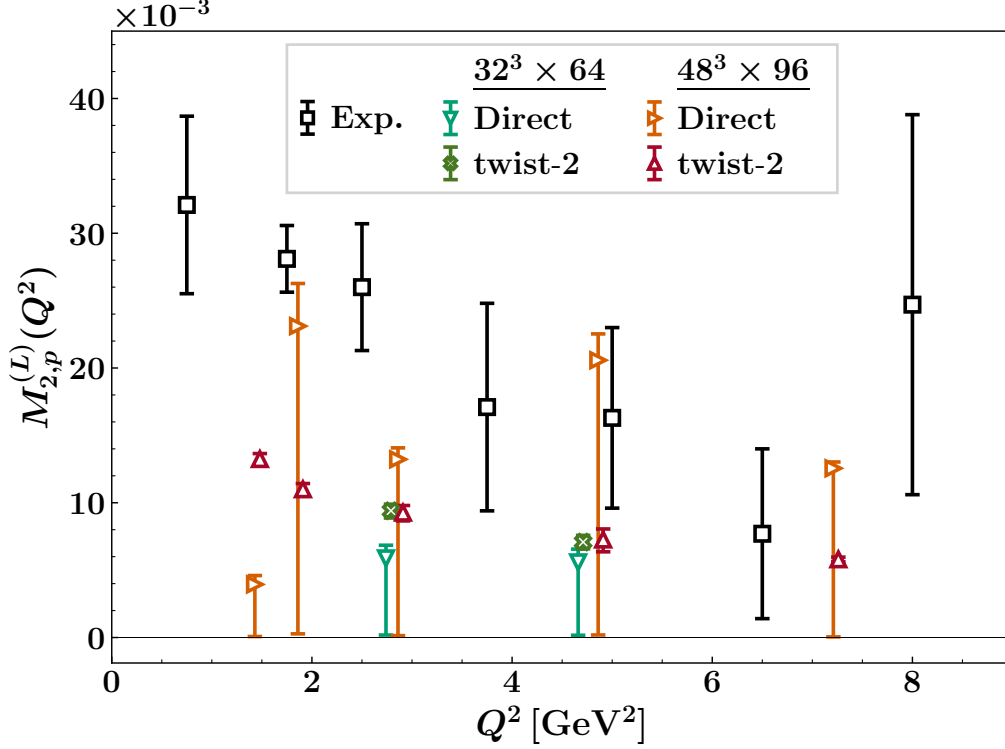


**Figure 5:**  $Q^2$  dependence of the lowest moments of proton  $F_L$  (Direct). Open squares are the experimental Nachtmann moments of  $F_L$  [30]. We also show the moments (twist-2) determined via the relation, Equation (44). Twist-2 points are displaced for clarity. Figure taken from [25].

Finally, in Figure 6 we show the  $uu$  and  $dd$  pieces of the polarised  $\mathcal{G}_1$  Compton structure function, along with the isovector  $uu - dd$  combination, as a function of  $\omega$ . We extract the first few Mellin moments using Equation (14) by following the same Bayesian analysis performed for the unpolarised case. Shaded bands in Figure 6 depict the resulting fits.

The lowest moment of  $g_1$  is a particularly interesting phenomenological quantity. It is directly related to the matrix elements of the axial current at leading-twist. For instance, the leading-twist contribution of the lowest isovector moment  $\tilde{M}_{2,uu-dd}^{(1)}$  provides a complementary approach to determining the nucleon isovector axial charge  $g_A$  via the Bjorken sum rule [32, 33], or alternatively, the QCD effective charge [34, 35]. However, our current results on polarised structure functions are very preliminary. They are obtained on a single ensemble at a single photon virtuality,  $Q^2 \sim 4.9 \text{ GeV}^2$  with limited statistics in an exploratory simulation. Although these are encouraging results, more progress is needed.

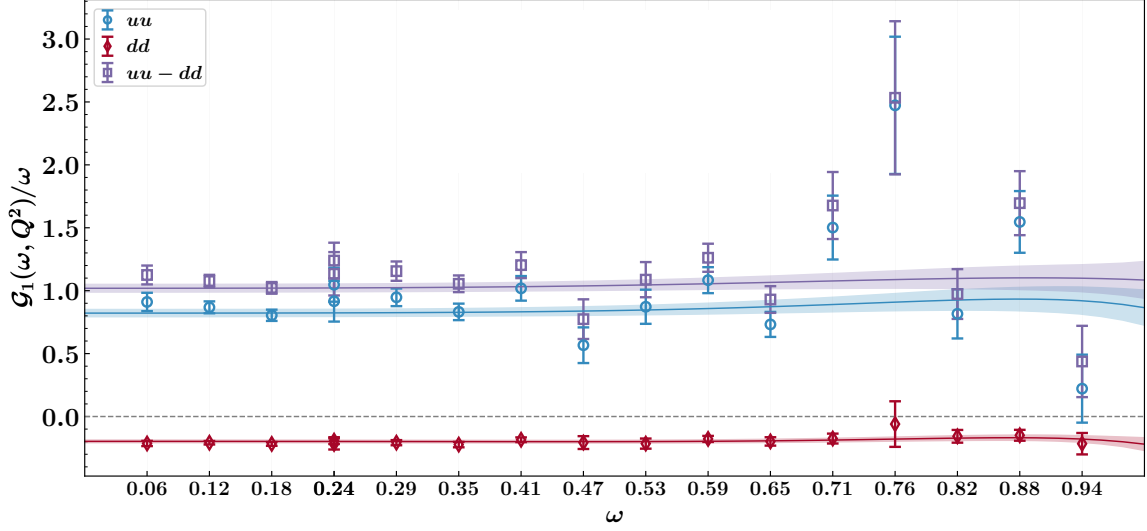


**Figure 6:** The polarised Compton structure function  $\mathcal{G}_1(\omega, Q^2)/\omega$  as a function of  $\omega$ . We show the preliminary result obtained on the  $48^3 \times 96$  ensemble at  $Q^2 \sim 4.9 \text{ GeV}^2$ .

## 7. Summary and outlook

The Compton amplitude approach has reached a certain maturity where it is possible to directly investigate the structure functions including the effects beyond leading twist. We have overviewed the relations between the forward Compton amplitude and the structure functions, and described a novel extension of the Feynman-Hellmann techniques that simplifies the calculation of the amplitude. We showed the versatility of this approach by calculating the moments of transverse and longitudinal proton structure functions along with their  $Q^2$  dependence. This allows us to study the power corrections for the first time in a lattice calculation. Currently our calculations involve configurations with two different lattice spacings and volumes, all at the  $SU(3)$  symmetric point. Calculations on additional ensembles that cover a range of lattice spacings and pion masses are required to fully account for systematic effects.

We are working towards extending our formalism to include the spin-dependent structure functions. Our preliminary results are encouraging. Additionally, accessing the parity violating structure function  $F_3$ , by considering weak currents is an exciting future direction.

## Acknowledgments

I thank the organisers of “The 39th International Symposium on Lattice Field Theory” for the invitation. I would also like to thank my colleagues from the QCDSF/UKQCD collaboration, this work would not have been possible without their contributions. The numerical configuration generation (using the BQCD lattice QCD program [36]) and data analysis (using the Chroma software library [37]) was carried out on the DiRAC Blue Gene Q and Extreme Scaling (EPCC, Edinburgh, UK) and Data Intensive (Cambridge, UK) services, the GCS supercomputers JUQUEEN and JUWELS (NIC, Jülich, Germany) and resources provided by HLRN (The North-German Supercomputer Alliance), the NCI National Facility in Canberra, Australia (supported by the

Australian Commonwealth Government) and the Phoenix HPC service (University of Adelaide). KUC is supported by the Australian Research Council grants DP190100297 and DP220103098. For the purpose of open access, the authors have applied a Creative Commons Attribution (CC BY) licence to any Author Accepted Manuscript version arising from this submission.

## References

- [1] G. Martinelli and C.T. Sachrajda, *On the difficulty of computing higher twist corrections*, *Nucl. Phys. B* **478** (1996) 660 [[hep-ph/9605336](#)].
- [2] X. Ji, *Parton Physics on a Euclidean Lattice*, *Phys. Rev. Lett.* **110** (2013) 262002 [[1305.1539](#)].
- [3] H.-W. Lin et al., *Parton distributions and lattice QCD calculations: a community white paper*, *Prog. Part. Nucl. Phys.* **100** (2018) 107 [[1711.07916](#)].
- [4] K. Cichy and M. Constantinou, *A guide to light-cone PDFs from Lattice QCD: an overview of approaches, techniques and results*, *Adv. High Energy Phys.* **2019** (2019) 3036904 [[1811.07248](#)].
- [5] M. Constantinou, *The  $x$ -dependence of hadronic parton distributions: A review on the progress of lattice QCD*, *Eur. Phys. J. A* **57** (2021) 77 [[2010.02445](#)].
- [6] K. Cichy, *Progress in  $x$ -dependent partonic distributions from lattice QCD*, *PoS LATTICE2021* (2022) 017 [[2110.07440](#)].
- [7] G.C. Rossi and M. Testa, *Note on lattice regularization and equal-time correlators for parton distribution functions*, *Phys. Rev. D* **96** (2017) 014507 [[1706.04428](#)].
- [8] V.M. Braun, A. Vladimirov and J.-H. Zhang, *Power corrections and renormalons in parton quasidistributions*, *Phys. Rev. D* **99** (2019) 014013 [[1810.00048](#)].
- [9] M. Göckeler, R. Horsley, D. Pleiter, P.E.L. Rakow, A. Schäfer, G. Schierholz et al., *Investigation of the second moment of the nucleon's  $g_1$  and  $g_2$  structure functions in two-flavor lattice QCD*, *Phys. Rev. D* **72** (2005) 054507 [[hep-lat/0506017](#)].
- [10] S. Bhattacharya, K. Cichy, M. Constantinou, A. Metz, A. Scapellato and F. Steffens, *Insights on proton structure from lattice QCD: The twist-3 parton distribution function  $g_T(x)$* , *Phys. Rev. D* **102** (2020) 111501 [[2004.04130](#)].
- [11] S. Bhattacharya, K. Cichy, M. Constantinou, A. Metz, A. Scapellato and F. Steffens, *Parton distribution functions beyond leading twist from lattice QCD: The  $h_L(x)$  case*, *Phys. Rev. D* **104** (2021) 114510 [[2107.02574](#)].
- [12] A.J. Chambers, R. Horsley, Y. Nakamura, H. Perlt, P.E.L. Rakow, G. Schierholz et al., *Nucleon structure functions from operator product expansion on the lattice*, *Phys. Rev. Lett.* **118** (2017) 242001.
- [13] R. Horsley, Y. Nakamura, H. Perlt, P.E.L. Rakow, G. Schierholz, K. Somfleth et al., *Structure functions from the Compton amplitude*, in *37th International Symposium on Lattice Field Theory (Lattice 2019) Wuhan, Hubei, China, June 16-22, 2019*, 2020 [[2001.05366](#)].
- [14] A. Hannaford-Gunn, K.U. Can, R. Horsley, Y. Nakamura, H. Perlt, P.E.L. Rakow et al., *Generalized parton distributions from the off-forward Compton amplitude in lattice QCD*, *Phys. Rev. D* **105** (2022) 014502 [[2110.11532](#)].

- [15] A. Hannaford-Gunn, R. Horsley, H. Perlt, P. Rakow, G. Schierholz, H. Stüben et al., *Generalised Parton Distributions from Lattice Feynman-Hellmann Techniques*, *PoS LATTICE2021* (2022) 088 [[2202.03662](#)].
- [16] A. Hannaford-Gunn, *A lattice QCD calculation of the off-forward Compton amplitude and generalised parton distributions, contribution to The 39th International Symposium on Lattice Field Theory, Bonn, Germany* (2021) .
- [17] A. Walker-Loud, C.E. Carlson and G.A. Miller, *The Electromagnetic Self-Energy Contribution to  $M_p - M_n$  and the Isovector Nucleon Magnetic Polarizability*, *Phys. Rev. Lett.* **108** (2012) 232301 [[1203.0254](#)].
- [18] F. Hagelstein and V. Pascalutsa, *The subtraction contribution to muonic-hydrogen Lamb shift: a point for lattice QCD calculation of polarizability effect*, [2010.11898](#).
- [19] J. Lozano, A. Agadjanov, J. Gegelia, U.G. Meißner and A. Rusetsky, *Finite volume corrections to forward Compton scattering off the nucleon*, *Phys. Rev. D* **103** (2021) 034507 [[2010.10917](#)].
- [20] A. Hannaford-Gunn et al., *Investigating the Compton amplitude subtraction function in lattice QCD*, *PoS LATTICE2021* (2022) 028 [[2207.03040](#)].
- [21] K.U. Can, A. Hannaford-Gunn, R. Horsley, Y. Nakamura, H. Perlt, P.E.L. Rakow et al., *Lattice QCD evaluation of the Compton amplitude employing the Feynman-Hellmann theorem*, *Phys. Rev. D* **102** (2020) 114505 [[2007.01523](#)].
- [22] A.J. Chambers, R. Horsley, Y. Nakamura, H. Perlt, D. Pleiter, P.E.L. Rakow et al., *Disconnected contributions to the spin of the nucleon*, *Phys. Rev. D* **92** (2015) 114517 [[1508.06856](#)].
- [23] W. Bietenholz et al., *Tuning the strange quark mass in lattice simulations*, *Phys. Lett.* **B690** (2010) 436 [[1003.1114](#)].
- [24] W. Bietenholz, V. Bornyakov, M. Göckeler, R. Horsley, W.G. Lockhart, Y. Nakamura et al., *Flavour blindness and patterns of flavour symmetry breaking in lattice simulations of up, down and strange quarks*, *Phys. Rev. D* **84** (2011) 054509 [[1102.5300](#)].
- [25] M. Batelaan et al., *Moments and power corrections of longitudinal and transverse proton structure functions from lattice QCD*, [2209.04141](#).
- [26] C.S. Armstrong, R. Ent, C.E. Keppel, S. Liuti, G. Niculescu and I. Niculescu, *Moments of the proton  $F_2$  structure function at low  $Q^2$* , *Phys. Rev. D* **63** (2001) 094008 [[hep-ph/0104055](#)].
- [27] C.E. Carlson and N.C. Mukhopadhyay, *Bloom-Gilman duality in the resonance spin structure functions*, *Phys. Rev. D* **58** (1998) 094029 [[hep-ph/9801205](#)].
- [28] W. Melnitchouk, *Local duality predictions for  $x \sim 1$  structure functions*, *Phys. Rev. Lett.* **86** (2001) 35 [[hep-ph/0106073](#)].
- [29] O. Nachtmann, *Positivity constraints for anomalous dimensions*, *Nuclear Physics B* **63** (1973) 237 .
- [30] P. Monaghan, A. Accardi, M.E. Christy, C.E. Keppel, W. Melnitchouk and L. Zhu, *Moments of the longitudinal proton structure function  $F_L$  from global data in the  $Q^2$  range 0.75-45.0 (GeV/c)<sup>2</sup>*, *Phys. Rev. Lett.* **110** (2013) 152002 [[1209.4542](#)].
- [31] G. Altarelli and G. Martinelli, *Transverse momentum of jets in electroproduction from*



- quantum chromodynamics, *Physics Letters B* **76** (1978) 89 .
- [32] A.V. Manohar, *An Introduction to spin dependent deep inelastic scattering*, in *Lake Louise Winter Institute: Symmetry and Spin in the Standard Model Lake Louise, Alberta, Canada, February 23-29, 1992*, pp. 1–46, 1992 [[hep-ph/9204208](#)].
  - [33] S.A. Larin and J.A.M. Vermaseren, *The  $\alpha_s^3$  corrections to the Bjorken sum rule for polarized electroproduction and to the Gross-Llewellyn Smith sum rule*, *Phys. Lett. B* **259** (1991) 345.
  - [34] A. Deur, S.J. Brodsky and G.F. de Teramond, *The QCD Running Coupling*, *Nucl. Phys.* **90** (2016) 1 [[1604.08082](#)].
  - [35] A. Deur, V. Burkert, J.P. Chen and W. Korsch, *Experimental determination of the QCD effective charge  $\alpha_{g_1}(Q)$* , *Particles* **5** (2022) 171 [[2205.01169](#)].
  - [36] T.R. Haar, Y. Nakamura and H. Stuben, *An update on the BQCD Hybrid Monte Carlo program*, *EPJ Web Conf.* **175** (2018) 14011 [[1711.03836](#)].
  - [37] R.G. Edwards and B. Joo, *The Chroma software system for lattice QCD*, *Nucl.Phys.Proc.Suppl.* **140** (2005) 832 [[hep-lat/0409003](#)].